nature geoscience

LETTERS

PUBLISHED ONLINE: 3 AUGUST 2014 | DOI: 10.1038/NGEO2220

Brownness of organics in aerosols from biomass burning linked to their black carbon content

Rawad Saleh[1], Ellis S. Robinson[1], Daniel S. Tkacik[1], Adam T. Ahern[1], Shang Liu[2], Allison C. Aiken[2], Ryan C. Sullivan[1], Albert A. Presto[1], Manvendra K. Dubey[2], Robert J. Yokelson[3], Neil M. Donahue[1] and Allen L. Robinson[1]*

Atmospheric particulate matter plays an important role in the Earth's radiative balance. Over the past two decades, it has been established that a portion of particulate matter, black carbon, absorbs significant amounts of light and exerts a warming effect rivalling that of anthropogenic carbon dioxide[1,2]. Most climate models treat black carbon as the sole light-absorbing carbonaceous particulate. However, some organic aerosols, dubbed brown carbon and mainly associated with biomass burning emissions[3–6], also absorbs light[7]. Unlike black carbon, whose light absorption properties are well understood[8], brown carbon comprises a wide range of poorly characterized compounds that exhibit highly variable absorptivities, with reported values spanning two orders of magnitude[3–6,9,10]. Here we present smog chamber experiments to characterize the effective absorptivity of organic aerosol from biomass burning under a range of conditions. We show that brown carbon in emissions from biomass burning is associated mostly with organic compounds of extremely low volatility[11]. In addition, we find that the effective absorptivity of organic aerosol in biomass burning emissions can be parameterized as a function of the ratio of black carbon to organic aerosol, indicating that aerosol absorptivity depends largely on burn conditions, not fuel type. We conclude that brown carbon from biomass burning can be an important factor in aerosol radiative forcing.

Black carbon (BC) in atmospheric particulate matter is an important global warming agent (potentially second only to CO_2) with estimates of its direct radiative forcing (DRF) ranging between 0.17 and 1.48 W m^{-2} (ref. 2). The large uncertainty in BC DRF stems partly from the mismatch between BC light absorption (hence its DRF) estimated by climate models and that retrieved using remote sensing, with models usually reporting smaller values[2]. Open biomass burning contributes one-third of the global BC budget. Biomass burning is also a major source of organic aerosol (OA), contributing two-thirds of the global primary OA budget[2,12], which most climate models treat as purely scattering. The cooling due to this scattering offsets the warming by BC from biomass burning, resulting in negative net DRF for biomass burning emissions[13]. However, there is a growing body of evidence that biomass burning OA contains substantial amounts of light-absorbing brown carbon[3–6] (BrC), which can shift the net biomass burning DRF to positive values[14]. Neglecting absorption by biomass burning OA might lead to misattribution of observed atmospheric particulate matter absorption to BC, contributing to the discrepancy between models and observations. There are substantial uncertainties in quantifying the effect of BrC. A major obstacle is the very high variability in reported light absorption properties of biomass burning OA, often attributed to fuel type and burn conditions[4,6], which complicates their treatment in climate models.

In this study, we show that the least volatile fraction (extremely low-volatility organic compounds, ELVOC, defined in the volatility basis set[11] to have saturation concentration $<3\times10^{-4}$ μg m^{-3}) of biomass burning OA emitted during the Fire Laboratory at Missoula Campaign (FLAME 4) exhibits substantially larger light absorption efficiency than the low-volatility (LVOC) and semi-volatile (SVOC) organic fractions. We parameterize the effective OA absorptivity (the imaginary part of the refractive index k_{OA}) across a diverse set of fuel types and burn conditions using the BC-to-OA ratio of the emissions, which is a measure of the combustion conditions. The k_{OA} values derived here can be used in Mie theory calculations to quantify light absorption by biomass burning OA. As the BC-to-OA ratio is tracked in emission inventories[2,15], our parameterization for biomass k_{OA} can be implemented in current large-scale chemical transport and climate models, provided our findings extend to open burning in general beyond FLAME 4.

We conducted experiments to characterize the effective k_{OA} in emissions of globally important fuels (Supplementary Section 1). The experiments spanned a broad range of burn conditions, OA loadings and chemical ageing processes (Supplementary Table 1). Dilute emissions were characterized and chemically aged in a smog chamber, replicating plume- and ambient-like conditions.

We performed optical closure, which combines real-time observations of size distributions and optical properties with Mie theory calculations, to retrieve the effective k_{OA} (ref. 6). Mie theory is widely used to model light absorption/scattering by atmospheric aerosols[16], and analyse experimental data and field measurements[5,17]. These calculations often assume a spherical core–shell morphology, which is clearly an approximation given the complex mixing state (fraction of OA internally mixed with BC, that is, exists with BC in the same particles) and morphology of BC and OA particles, which is under debate[5,17–19]. If the OA exist as a coating over the BC, it can enhance BC absorption by refracting light into the BC core (lensing[20,21]). In this study, we retrieve k_{OA} using two limiting cases: (1) BC and OA are completely externally mixed (they exist in different particles); and (2) a fraction of the OA is internally mixed with and exists as a coating over the BC, with maximum possible coating thickness (Supplementary Section 2). We note that from a light-absorption perspective, case (1) also corresponds to

[1]Center for Atmospheric Particle Studies, Carnegie Mellon University, Pittsburgh, Pennsylvania 15213, USA, [2]Earth and Environmental Sciences, Los Alamos National Laboratory, Los Alamos, New Mexico 87545, USA, [3]Department of Chemistry, University of Montana, Missoula, Montana 59812, USA. *e-mail: alr@andrew.cmu.edu

BC and OA being internally mixed, but BC residing on the edge of the particle rather than being coated by OA (ref. 18). For the conditions of our experiments, and biomass burning emissions in general, we expect case (2) to better approximate the mixing state and morphology of BC and OA. BC particles form initially during combustion, and as the emissions temperature drops, organic vapours hit supersaturation and are forced by the second law of thermodynamics to condense (form OA). The BC particles provide surface area that facilitates condensation; thus, whenever condensable organic molecules encounter BC particles, they would prefer to condense on them rather than form new (externally mixed) particles by nucleation. Given the large OA loadings in most of the experiments (Supplementary Table 1), we expect OA to form relatively thick coatings over BC.

As described in Supplementary Section 3, the internally mixed case (case 2) yields smaller k_{OA} values than the externally mixed case (case 1). However, the main conclusions of this work (summarized in Figs 1 and 2 for the internally mixed case and Supplementary Figs 1 and 2 for the externally mixed case), discussed below, hold for both cases. Furthermore, owing to uncertainty in BC mass concentration measurements, the analysis presented here is based on the limiting case of maximum possible BC concentration, which corresponds to a lower limit on the derived k_{OA} values (see Supplementary Section 3 for details). Thus, k_{OA} values presented in this study should be viewed as lower bound values.

Figure 1a,b shows the effective absorptivity at wavelength (λ) of 550 nm ($k_{OA,550}$) and the wavelength dependence of k_{OA} (w; where $k_{OA} = k_{OA,550} \times (550/\lambda)^{w}$) as a function of BC-to-OA ratio of the emissions. The wavelength dependence of absorption is often described using the absorption Ångström exponent (AAE). For small particles (<50 nm) in the visible spectrum AAE $= w + 1$. For example, the imaginary part of the refractive index of BC is wavelength independent in the visible spectrum[8] ($w = 0$), and AAE $\cong$ 1. The k_{OA} values reported here are the absorptivity of OA alone, excluding the contribution from BC.

Figure 1a,b indicates that, regardless of fuel type, $k_{OA,550}$ increases with the BC-to-OA ratio, whereas w is inversely proportional to BC-to-OA ratio. Therefore, k_{OA} depends strongly on burn conditions, which, to a large extent, dictate the BC-to-OA ratio. As evident from the multiple experiments for black spruce and ponderosa pine, the OA emitted by the same fuel had different k_{OA} when the BC-to-OA ratios were different. Thus, biomass fuel type had no discernible effect on k_{OA} beyond the BC-to-OA ratio. We note that although k_{OA} depends on BC-to-OA ratio and not fuel type, certain fuels often exhibit characteristic BC-to-OA ratios. For example, grass fires, which tended to be flaming, had larger BC-to-OA ratios than boreal fires, which tended to be more smoldering[22].

The BC-to-OA ratio also depends, although to a lesser extent, on OA loading and secondary OA (SOA) formation. Both phenomena affect k_{OA} in a fashion consistent with the trend shown in Fig. 1. As the OA loading increases, the BC-to-OA ratio decreases because more SVOCs partition to the condensed phase[23], thus reducing the effective $k_{OA,550}$ (Supplementary Fig. 3). SOA formation has a similar effect because it reduces the BC-to-OA ratio. SOA is less absorptive than primary OA, but has a stronger wavelength dependence[6], potentially decreasing $k_{OA,550}$ and increasing w. This is not clearly observed in some of the experiments because the effect of SOA addition is comparable to measurement uncertainties, but the aged aerosol still falls on the same trend as the fresh aerosol, as shown in Fig. 1a,b.

The observed dependence of k_{OA} on BC-to-OA ratio seems to apply solely to biomass burning OA. In Fig. 1a,b, we also plot data for diesel engine emissions. For similar BC-to-OA ratios, diesel k_{OA} values are several-fold smaller than biomass burning values. There is no relationship between the diesel k_{OA} and the BC-to-OA ratio. This demonstrates that the dependence of k_{OA} on BC-to-OA ratio for biomass burning emissions is not an artefact of the optical closure analysis.

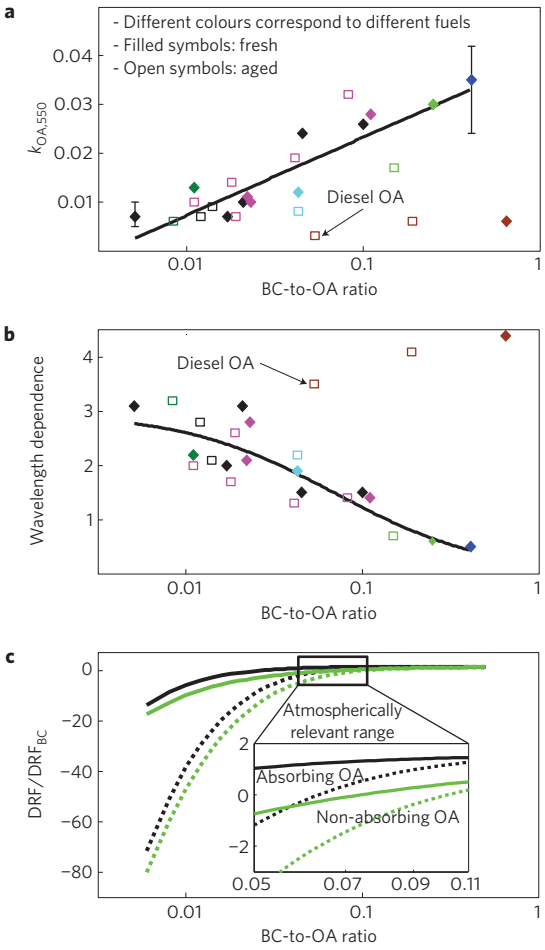

Figure 1 | Dependence of k_{OA} and DRF on BC-to-OA ratio. a,**b**, Filled diamonds and open squares correspond to fresh and chemically aged emissions, respectively. Colours correspond to different fuels: black, black spruce; magenta, ponderosa pine; cyan, rice straw; forest green, organic hay; light green, saw grass; blue, wire grass; and brown, diesel. Whiskers represent upper and lower bounds (Supplementary Section 3). Black lines are least-squares fits to the biomass burning data: $y = 0.016x + 0.03925$, R-square = 0.734, for $k_{OA,550\,nm}$ versus $\log_{10}$(BC-to-OA ratio), **a** and $y = 0.2081/(x + 0.0699)$, R-square = 0.738, for w versus BC-to-OA ratio, **b**. **c**, Ratio of DRF of biomass burning emissions to DRF of biomass burning BC alone. Black lines use k_{OA} values obtained in this study. Green lines assume non-absorbing OA ($k_{OA} = 0$). Solid lines: coating thickness was held constant, and the concentration of externally mixed OA varied in the BC-to-OA ratio space; dotted lines: the fractions of internally and externally mixed OA were held constant at 50%, while the coating thickness varied (see Supplementary Section 7 for details).

We performed thermodenuder measurements in a subset of the experiments (Supplementary Table 2) to characterize k_{OA} as a function of volatility. Heating at 250 °C stripped LVOCs and SVOCs (77–91% of original particulate matter mass) from the particles, leaving BC (1–10% of original particulate matter mass) and ELVOCs (7–14% of original particulate matter mass). As shown in Fig. 2b, k_{OA} values of the ELVOCs (retrieved from the heated measurements) are an order of magnitude larger than the k_{OA} values of the total OA (retrieved from the non-heated measurements). This indicates that almost all of the OA absorption was associated with ELVOCs.

The dependence of k_{OA} on BC-to-OA ratio supports the conclusion that ELVOCs are an order of magnitude more absorptive

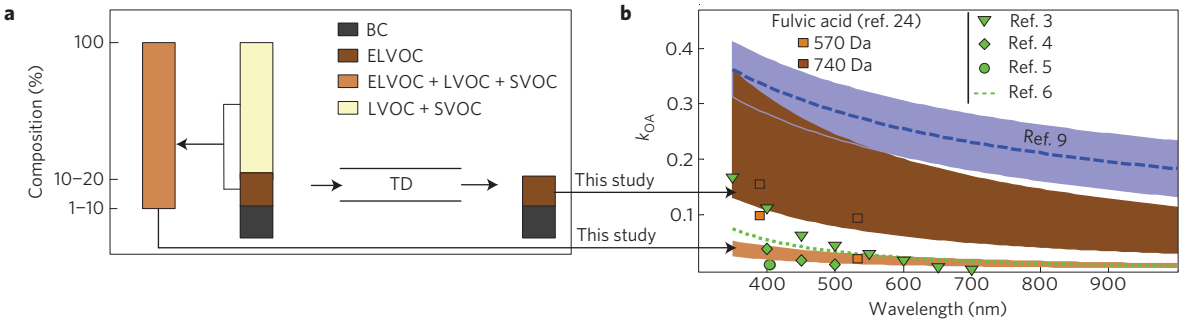

Figure 2 | Contribution of different OA components to light absorption. a, Composition of the condensed-phase emissions in the experiments that involved heating in the thermodenuder (TD). **b**, The range of k_{OA} as a function of wavelength for the total OA (light brown shade) and ELVOCs (dark brown shade). Green dotted line and symbols correspond to k_{OA} values reported in the literature for biomass burning emissions excluding those of ref. 9 (dashed blue line; the blue shaded area is the uncertainty bound). Light and dark brown squares correspond to bulk (nominal molecular mass of 570 Da) and the fraction with largest molecular mass (740 Da) of fulvic acid[24].

than the total OA (ELVOCs + LVOCs + SVOCs). We propose a mechanism in which the conditions leading to BC formation (an oxygen-deprived, fuel-rich flame) are also conducive to formation of large organic compounds that have very low volatility and are highly absorbing. Consequently, the higher the BC content of the emissions, the larger is the effective OA absorptivity. As this dependence is not observed in diesel emissions (Fig. 1), clearly, fuel composition (a mixture of liquid hydrocarbons in diesel versus large polymers in biomass) and combustion conditions (high pressure in diesel engine versus heat breaking down the solid fuel at atmospheric pressure in biomass burning) are important factors. The dependence of absorptivity on volatility observed here is consistent with the work of a previous study[24], which found that the absorptivity of fulvic acid components increased with increasing molecular weight, hence decreasing volatility (Fig. 2b).

ELVOCs having k_{OA} an order of magnitude larger than the total OA explains the seemingly discordant very large k_{OA} reported in ref. 9 for aged biomass burning particles. That study used transmission electron microscopy, where particles were exposed to vacuum and bombarded with a high-energy electron beam. In such an environment, as in the thermodenuder, LVOCs and SVOCs are expected to evaporate (Supplementary Fig 4), leaving only the highly absorptive ELVOCs in the condensed phase. As shown in Fig. 2b, our k_{OA} values for ELVOCs are in close agreement with those of ref. 9, and k_{OA} values for our total OA are in good agreement with data collected using ambient pressure techniques[3–6].

To illustrate the potential climate forcing implications of our findings, we performed simplified calculations (Supplementary Section 7) to estimate the contribution of biomass burning OA to DRF. Results are shown in Fig. 1c. BC-to-OA ratios between 0.05 and 0.1 are most relevant as they are representative of the mean global values for biomass burning[2]. Under these conditions, if the OA were non-absorbing, the DRF would be negative. This is in concordance with predictions of current climate models that do not treat BrC absorption[13]. BrC absorption, on the other hand, shifts DRF of biomass burning emissions to positive values. Although these are idealized calculations, they suggest that BrC in biomass burning emissions can be a major player alongside BC to govern DRF.

Methods

Experiments were conducted during FLAME 4 using globally important fuels from boreal forests, grasslands and croplands (Supplementary Table 1). Emissions were diluted to plume- and ambient-like concentrations and injected into two smog chambers[25]. In one of the chambers, the emissions were chemically aged by photo-oxidation or dark ozonolysis, whereas the second chamber served as a control (no oxidation). The ageing time in the chambers was of the order of 1–3 h (Supplementary Fig. 7). For the photo-oxidation experiments, the OH concentration was similar to atmospheric conditions ($\sim 2 \times 10^6$ molecules cm^{-3}), whereas for ozonolysis, the ozone concentrations ($\sim$1 ppm) were 2 orders of magnitude larger than typical atmospheric and biomass burning plume ozone concentrations ($\sim$10–50 ppb). Thus, the ageing time in the ozonolysis experiments was equivalent to a few days of atmospheric ageing. The experiments featured a wide range of burn conditions, which was reflected in the wide range of BC-to-OA ratios in the diluted emissions (Supplementary Table 1).

Effective absorptivity of OA, namely the imaginary part of the refractive index (k_{OA}), was retrieved using optical closure, which combines measurement of absorption coefficients, as well as BC and OA size distributions and mixing states, with Mie theory calculations[6] (Supplementary Section 2 and Fig. 4). The Mie theory absorption calculations were based on the formulation in ref. 26 for coated spheres. Optical closure was performed on both fresh and aged emissions. To investigate the volatility of BrC, some experiments also involved heating the emissions in a thermodenuder to 250 °C for an average residence time of 5.8 s. Heating stripped almost 90% of the OA, corresponding to the LVOC and SVOC fraction, from the condensed phase. The remaining ELVOC fraction has effective saturation concentration (C^*) less than 10^{-4} μg m^{-3} (Supplementary Fig. 8).

Further details of experimental set-up, instrumentation, data and uncertainty analysis are provided in the Supplementary Methods.

Received 23 February 2014; accepted 10 July 2014;
published online 3 August 2014

References

1. Ramanathan, V. & Carmichael, G. Global and regional climate changes due to black carbon. *Nature Geosci.* **1,** 221–227 (2008).
2. Bond, T. C. *et al.* Bounding the role of black carbon in the climate system: A scientific assessment. *J. Geophys. Res. Atmos.* **118,** 5380–5552 (2013).
3. Kirchstetter, T. W. & Novakov, T. Evidence that the spectral dependence of light absorption by aerosols is affected by organic carbon. *J. Geophys. Res.* **109,** 1–12 (2004).
4. Chen, Y. & Bond, T. C. Light absorption by organic carbon from wood combustion. *Atmos. Chem. Phys.* **10,** 1773–1787 (2010).
5. Lack, D. A., Langridge, J. M., Bahreini, R., Cappa, C. D. & Middlebrook, A. M. Brown carbon and internal mixing in biomass burning particles. *Proc. Natl Acad. Sci. USA* **109,** 14802–14807 (2012).
6. Saleh, R. *et al.* Absorptivity of brown carbon in fresh and photo-chemically aged biomass-burning emissions. *Atmos. Chem. Phys.* **13,** 7683–7693 (2013).
7. Andreae, M. O., Gelencs, A., Box, P. O. & Veszpr, H. Black carbon or brown carbon? The nature of light-absorbing carbonaceous aerosols. *Atmos. Chem. Phys.* **6,** 3131–3148 (2006).
8. Bond, T. C. & Bergstrom, R. W. Light absorption by carbonaceous particles: An investigative review. *Aerosol Sci. Technol.* **39,** 1–41 (2005).
9. Alexander, D. T. L., Crozier, P. A & Anderson, J. R. Brown carbon spheres in East Asian outflow and their optical properties. *Science* **321,** 833–836 (2008).
10. Chakrabarty, R. K. *et al.* Brown carbon in tar balls from smoldering biomass combustion. *Atmos. Chem. Phys.* **10,** 6363–6370 (2010).
11. Donahue, N. M., Kroll, J. H., Pandis, S. N. & Robinson, A. L. A two-dimensional volatility basis set—Part 2: Diagnostics of organic-aerosol evolution. *Atmos. Chem. Phys.* **12,** 615–634 (2012).
12. Bond, T. C. A technology-based global inventory of black and organic carbon emissions from combustion. *J. Geophys. Res.* **109,** 1–43 (2004).

13. Myhre, G. *et al.* Radiative forcing of the direct aerosol effect from AeroCom Phase II simulations. *Atmos. Chem. Phys.* **13,** 1853–1877 (2013).
14. Feng, Y., Ramanathan, V. & Kotamarthi, V. R. Brown carbon: A significant atmospheric absorber of solar radiation? *Atmos. Chem. Phys.* **13,** 8607–8621 (2013).
15. Wiedinmyer, C. *et al.* The Fire INventory from NCAR (FINN): A high resolution global model to estimate the emissions from open burning. *Geosci. Model Dev.* **4,** 625–641 (2011).
16. Jacobson, M. Z. Investigating cloud absorption effects: Global absorption properties of black carbon, tar balls, and soil dust in clouds and aerosols. *J. Geophys. Res.* **117,** D06205 (2012).
17. Cappa, C. D. *et al.* Radiative absorption enhancements due to the mixing state of atmospheric black carbon. *Science* **337,** 1078–1081 (2012).
18. Adachi, K., Chung, S. H. & Buseck, P. R. Shapes of soot aerosol particles and implications for their effects on climate. *J. Geophys. Res.* **115,** 1–9 (2010).
19. China, S., Mazzoleni, C., Gorkowski, K., Aiken, A. C. & Dubey, M. K. Morphology and mixing state of individual freshly emitted wildfire carbonaceous particles. *Nature Commun.* **4,** 2122 (2013).
20. Bond, T. C., Habib, G. & Bergstrom, R. W. Limitations in the enhancement of visible light absorption due to mixing state. *J. Geophys. Res.* **111,** 1–13 (2006).
21. Lack, D. A. & Cappa, C. D. Impact of brown and clear carbon on light absorption enhancement, single scatter albedo and absorption wavelength dependence of black carbon. *Atmos. Chem. Phys.* **10,** 4207–4220 (2010).
22. Akagi, S. K. *et al.* Emission factors for open and domestic biomass burning for use in atmospheric models. *Atmos. Chem. Phys.* **11,** 4039–4072 (2011).
23. May, A. A. *et al.* Gas-particle partitioning of primary organic aerosol emissions: (3) Biomass burning. *J. Geophys. Res.* **118,** 11327–11338 (2013).
24. Dinar, E. *et al.* The complex refractive index of atmospheric and model humic-like substances (HULIS) retrieved by a cavity ring down aerosol spectrometer (CRD-AS). *Faraday Discuss.* **137,** 279–295 (2008).
25. Hennigan, C. J. *et al.* Chemical and physical transformations of organic aerosol from the photo-oxidation of open biomass burning emissions in an environmental chamber. *Atmos. Chem. Phys.* **11,** 7669–7686 (2011).
26. Bohren, C. F. & Huffman, D. R. *Absorption and Scattering of Light by Small Particles* (Wiley, 1983).

Acknowledgements

FLAME 4 and R.J.Y. were supported by NSF grant ATM-0936321. S.L., A.C.A. and M.K.D. thank DOE's ASR programme F265 for financial support. Carnegie Mellon University team thanks DOE's ASR programme (ER65296) and NSF (AGS-1256042) for financial support. The authors also thank the Fire Science Laboratory Staff and other FLAME 4 team members.

Author contributions

R.S. performed the data analysis and wrote the manuscript. R.S., A.L.R., N.M.D., R.C.S. and A.A.P. designed the experiments. E.S.R., A.T.A., D.S.T. and R.S. performed smog chamber experiments. A.L.R., A.A.P., R.C.S., A.T.A., D.S.T., E.S.R. and R.S. built the smog chamber experimental set-up. E.S.R. analysed SP2 and HR-AMS data. S.L. and A.C.A. collected and analysed PASS-3 data. R.J.Y. organized FLAME 4. All authors discussed the data and commented on the manuscript.

Additional information

Supplementary information is available in the online version of the paper. Reprints and permissions information is available online at www.nature.com/reprints. Correspondence and requests for materials should be addressed to A.L.R.

Competing financial interests

The authors declare no competing financial interests.